Electrochemistry Communications 22 (2012) 128–132

Contents lists available at SciVerse ScienceDirect

Electrochemistry Communications

journal homepage: www.elsevier.com/locate/elecom

Nanocomposite of MoS_2 on ordered mesoporous carbon nanospheres: A highly active catalyst for electrochemical hydrogen evolution

Xiaojun Bian [a], Jie Zhu [a], Lei Liao [a], Micheál D. Scanlon [b], Peiyu Ge [b], Chang Ji [c], Hubert H. Girault [b], Baohong Liu [a,*]

[a] Department of Chemistry and State Key Lab of Molecular Engineering of Polymers, Fudan University, Shanghai 200433, China
[b] Laboratoire d'Electrochimie Physique et Analytique, EPFL, CH-1015 Lausanne, Switzerland
[c] Department of Chemistry and Biochemistry, Texas State University, San Marcos, Texas 78666, USA

ARTICLE INFO

Article history:
Received 15 May 2012
Received in revised form 3 June 2012
Accepted 7 June 2012
Available online 15 June 2012

Keywords:
Electrocatalyst
Hydrogen evolution reaction
Mesoporous carbon nanospheres
Molybdenum disulfide

ABSTRACT

An efficient electrocatalyst for hydrogen evolution has been developed based upon in situ reduction of MoS_2 on ordered mesoporous carbon nanospheres (MoS_2/MCNs). The properties of MoS_2/MCNs were characterised by scanning electron microscopy, transmission electron microscopy and X-ray photoelectron spectroscopy. Polarisation curves and electrochemical impedance measurements were obtained for MoS_2/MCNs modified glassy carbon electrodes. The MoS_2/MCNs exhibit high catalytic activity for hydrogen evolution with a low overpotential and a very high current density. A theory outlining the origins of the Tafel slope for a Volmer-Heyrovsky (rate determining step) mechanism of hydrogen evolution at MoS_2 catalytic edge sites is presented.

1. Introduction

Developing technology to satisfy global energy demand in an economical and environmentally friendly manner is a pressing challenge facing the scientific community. Hydrogen evolution reaction (HER), whereby aqueous protons are reduced to hydrogen, is of vital technological importance for future carbon-neutral energy production [1–3].

The electrocatalytic HER is catalyzed most effectively by Pt group metals [4–9]. However, large scale applications of Pt catalysts have been restricted due to their high cost and low abundance. Thus, it is desirable to find new efficient hydrogen evolution catalysts (HECs), preferably based on cheap, non-toxic, stable and abundant materials. Molybdenum sulfides (MoS_x), which have biomimetic structures analogous to nitrogenase active sites, initially attracted extensive interest as HECs following pioneering work by Tributsch and Bennett [10]. Recently, interest has been rekindled by Nørskov's group who highlighted, by density function theory (DFT) calulations, that MoS_2's hydrogen binding energy is similar to that of Pt [5,11].

To date, two key strategies have been applied to develop highly active MoS_2-based HECs. The first is to increase the amount of sulphur active edge sites of MoS_2 plates [7,12]. A second strategy is to improve the electronic contact between the active sites and the underlying electrode. From this viewpoint, carbon materials are good candidates to support catalysts due to their unique physicochemical properties. MoS_2 loaded on graphene, graphite, and carbon nanotubes have been used as catalysts for hydrodesulfurization catalysis [13], lithium ion batteries [14,15] and HER [11,16]. The electrocatalytic activity of MoS_2 mainly depends on the morphology and electrical coupling of the catalysts. In this regard, forming highly dispersed nanoparticulate (i.e., edge rich) MoS_2 on a conducting matrix is an ideal protocol to lower the activation potential for HER.

Ordered mesoporous carbon materials have been employed as advanced matrices in biosensing research [17,18], benefiting from their high specific surface area, large pore volume, and adjustable mesopores. In this work, a highly active MoS_2/MCNs catalyst based on MoS_2 uniformly distributed on ordered mesoporous carbon nanospheres, ~100 nm in size, has been prepared *via* an in situ reduction method. Studies show that the nanocomposites possess an excellent electrocatalytic activity for HER with a low overpotential and a high current density.

2. Experimental

2.1. Reagents

$(NH_4)_2MoS_4$ (99.97%), hydrazine monohydrate (98%), and Nafion® perfluorinated ion-exchange resin solution (5% w/w) were purchased

* Corresponding author. Fax: +86 21 6564 1740.
E-mail address: bhliu@fudan.edu.cn (B. Liu).

1388-2481/$ – see front matter © 2012 Elsevier B.V. All rights reserved.
doi:10.1016/j.elecom.2012.06.009

from Sigma-Aldrich. Dimethylformamide (DMF, ≥99.5%) and ethanol were obtained from the Shanghai Chemical Plant.

2.2. Synthesis of MoS_2/MCNs catalyst

MCNs were prepared according to Zhao's method [19]. MoS_2/MCNs with different Mo/C molar ratios were prepared by a one-step hydrothermal method [16]. 10 mg of MCNs were dispersed in 10 mL of DMF via sonication. An amount of $(NH_4)_2MoS_4$, corresponding to the desired Mo/C ratio, and 0.1 mL of $N_2H_4 \cdot H_2O$ were then added to the suspension. The solution was transferred to a 40 mL autoclave and kept at 200 °C for 12 h. Subsequently, the reaction mixture was centrifuged and washed with copious water. The final product was collected after lyophilization.

2.3. Characterisation techniques

Scanning electron microscopy (SEM) images were recorded by a JEOL 6400 microscope operated at 10 keV. Transmission electron microscopy (TEM) studies were carried out using a JEOL JEM-2011 electron microscope at an acceleration voltage of 200 keV. The Mo/C molar ratios were measured by inductively coupled plasma (ICP) using an IRIS Intrepid instrument. X-ray photoelectron spectroscopic (XPS) analysis was performed on a Perkin-Elmer PHI 5000 C spectrometer using Mg Kα

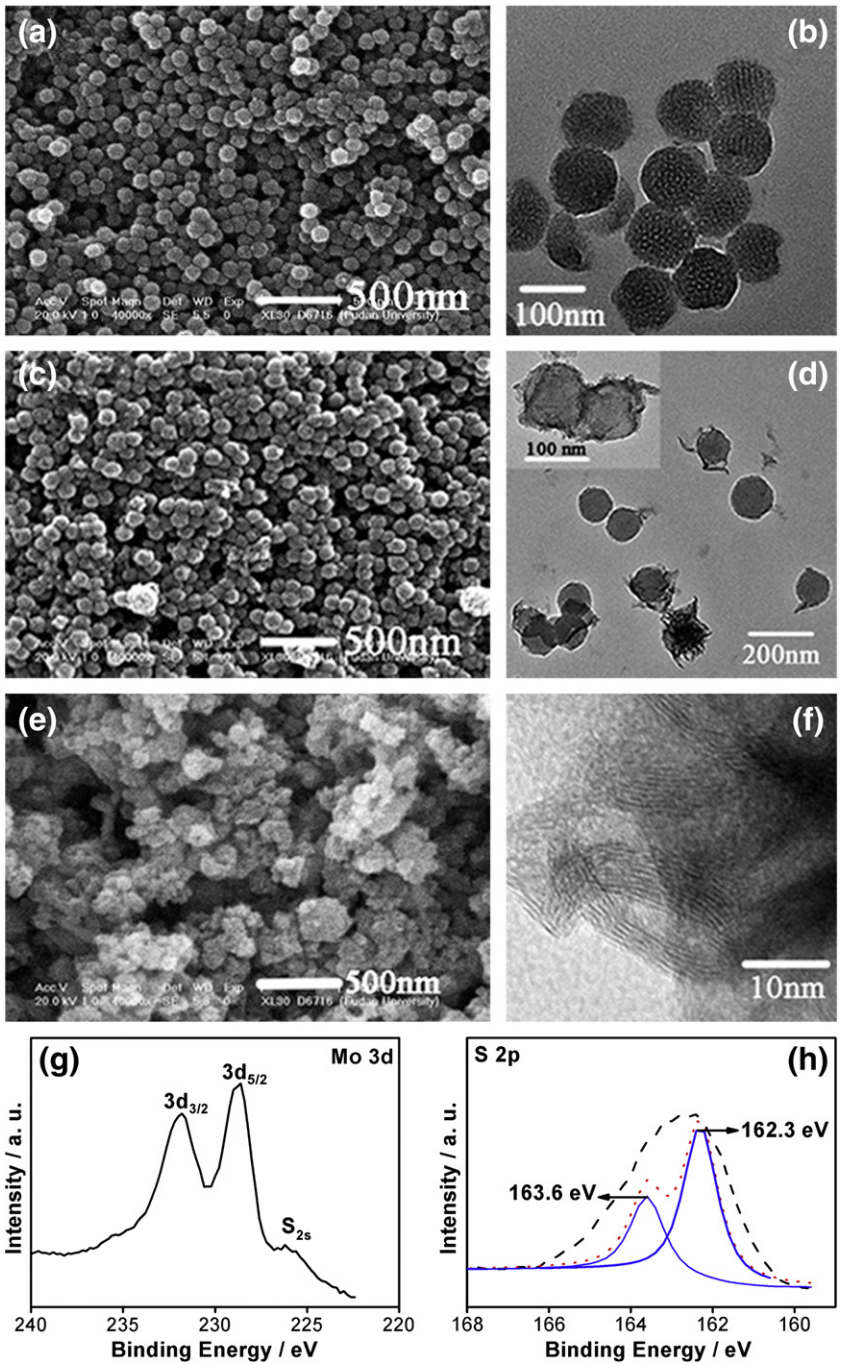

Fig. 1. SEM images of (a) MCNs, (c) MoS_2/MCNs, and (e) pure MoS_2. TEM images of (b) MCNs and (d) MoS_2/MCNs with Mo/C molar ratio of 0.05. (f) High-magnification TEM of layered MoS_2 grown on MCNs. XPS spectra of MoS_2/MCNs showing (g) Mo 3d and S 2 s peaks and (h) S 2p peaks.

radiation (1253.6 eV with pass energy of 20.0 eV). The carbonaceous C 1 s line (284.6 eV) was used as the reference to calibrate the binding energies.

2.4. Preparation of MoS_2-modified electrodes and electrochemical studies

3.8 mg of MoS_2/MCNs (Mo/C = 0.05) was dispersed in 0.5 mL of a solution composed of 4:1 (v/v) distilled water and ethanol containing 0.5% (w/w) Nafion. Subsequently, an amount of the catalyst slurry was pipetted on the surface of a GCE (3.5 mm in diameter) with a catalyst loading of 0.19 mg/cm^2. The modified GCE (MoS_2/MCNs-GCE) was left to dry at room temperature. Each modified electrode was prepared with an identical MoS_2 loading.

All electrochemical studies were performed using a PGSTAT potentiostat (Eco-Chemie, Netherlands) in a standard three-electrode setup. The electrocatalytic activity of MoS_2/MCNs towards HER was examined using linear sweep voltammetry (LSV). Electrochemical impedance spectroscopic (EIS) measurements were carried out in 0.5 M H_2SO_4 in the frequency range 10^{-2} to 10^6 Hz with a single modulated AC potential of 10 mV.

3. Results and discussion

3.1. Characterisation of MoS_2/MCNs nanocomposites

MoS_2/MCNs were prepared by a hydrothermal reaction of $(NH_4)_2MoS_4$ with hydrazine in DMF solution containing MCNs as the matrices, which have a large specific surface area of 719 m^2 g^{-1}, a volume capacity of 0.98 cm^3 g^{-1}, and a narrow pore size of approximately 3 nm. During this process, the $(NH_4)_2MoS_4$ precursor was reduced to MoS_2, which homogeneously impregnated on MCNs.

SEM and TEM analysis, respectively, revealed a marked difference in the morphology of MoS_2 nanoparticles grown freely in solution in comparison to their growth in the presence of MCNs under otherwise identical conditions. Both MCNs (Fig. 1a, b) and MoS_2/MCNs (Fig. 1c, d) were distributed homogenously with a diameter of about 100 nm, indicating that MCNs could act as effective matrices for mediating the in situ growth of MoS_2 with a highly uniform dispersion. In contrast, pure MoS_2 nanoparticles would aggregate into particles a few hundred nanometers in size (Fig. 1e). High-magnification TEM (Fig. 1f) shows a series of parallel lines embedded in the surface of MCNs with each line corresponding to a layer of MoS_2. The resultant intimate contact between MCNs matrices and MoS_2 may further enhance the electron transfer and improve the electrocatalytic activity for HER.

The presence of MoS_2 on MCNs was also verified by XPS. The well-defined spin-coupled Mo and S doublets, highlighted in Fig. 1g, h, are at nearly the same binding energies as those for commercial MoS_2 nanoparticles [13]. Two strong peaks are observed at approximately 228.7 and 231.8 eV (Fig. 1g), which can be attributed to Mo 3d 5/2 and Mo 3d 3/2 binding energies, respectively. In Fig. 1h, the peaks at about 162.3 and 163.6 eV are related to S 2p 3/2 and S 2p 1/2 binding energies, respectively.

3.2. Optimisation and catalytic properties of MoS_2/MCN-modified electrodes

The Mo/C molar ratio in MoS_2/MCNs was optimised for hydrogen evolution. Given uniform loadings of catalyst on the electrode surface (0.19 mg/cm^2), Mo/C ratios of 0.05–0.075 showed better catalytic activity with higher current densities (j) (Fig. 2a, b). TEM images confirmed that lower molar ratios of Mo/C could induce the homogenous growth of nanosized MoS_2 on MCNs (Figs. 1d and 2c). While a higher molar ratio of Mo/C (0.1) may initiate the aggregation of MoS_2 on MCNs (Fig. 2d) and thereby inhibit the catalytic activity of MoS_2/MCNs.

A comparative study was undertaken whereby the catalytic activity of MoS_2/MCNs for HER was related to that of pure nanoparticles of

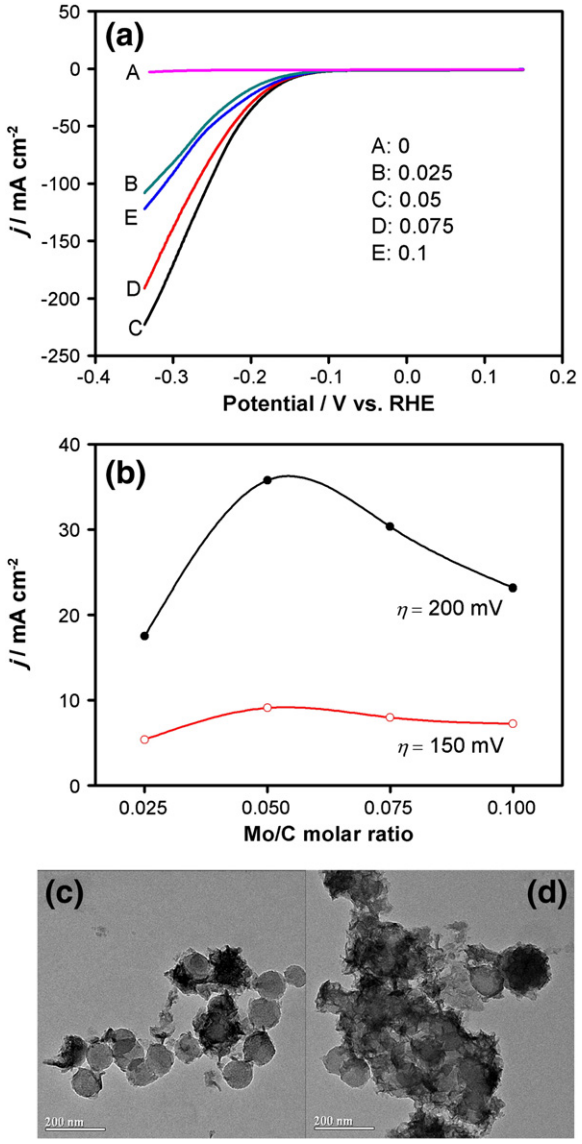

Fig. 2. (a) LSV polarisation curves for MoS_2/MCNs-GCEs with different molar ratios of Mo/C in 0.5 M H_2SO_4; scan rate: 2 mV/s. (b) Current densities for MoS_2/MCNs-GCEs with different molar ratios of Mo/C at overpotentials of 150 mV (hollow circles) and 200 mV (solid circles). TEM images of MoS_2/MCNs with Mo/C molar ratios of (c) 0.075 and (d) 0.1.

MoS_2, MCNs, and a physical mixture of MoS_2 and MCNs (MoS_2–MCNs) (Fig. 3). The MoS_2/MCNs-GCE exhibited the lowest onset potential at approximately −0.1 V (vs. RHE) for HER with high current densities of ~7 and ~30 mA/cm^2 at overpotentials of 150 and 200 mV, respectively. Catalytic activity, in terms of the HER onset potential and observed current densities, was much lower for pure MoS_2 and MoS_2–MCNs modified GCEs, while entirely absent for MCNs (Fig. 3a). The improved electrocatalysis exhibited by the MoS_2/MCNs-GCE suggests a smaller activation energy for HER. Nanoparticulate growth on MCNs is confined such that very small and thereby edge-rich, MoS_2 is formed in comparison to the large aggregated MoS_2 grown freely in solution. Additionally, the intimate coupling between MoS_2 and the highly conductive MCNs should permit extremely efficient electrical communication between the catalytic edge sites and underlying electrode. To further confirm this hypothesis, impedance measurements were carried out. The MoS_2/MCNs-GCE displayed the lowest faradaic impedance of the three electrodes (Fig. 3b). The resulting facile electron transfer between the electrode and MoS_2/MCNs with abundant catalytic edges sites facilitated the kinetics for HER. Furthermore, the MoS_2/MCN-modified

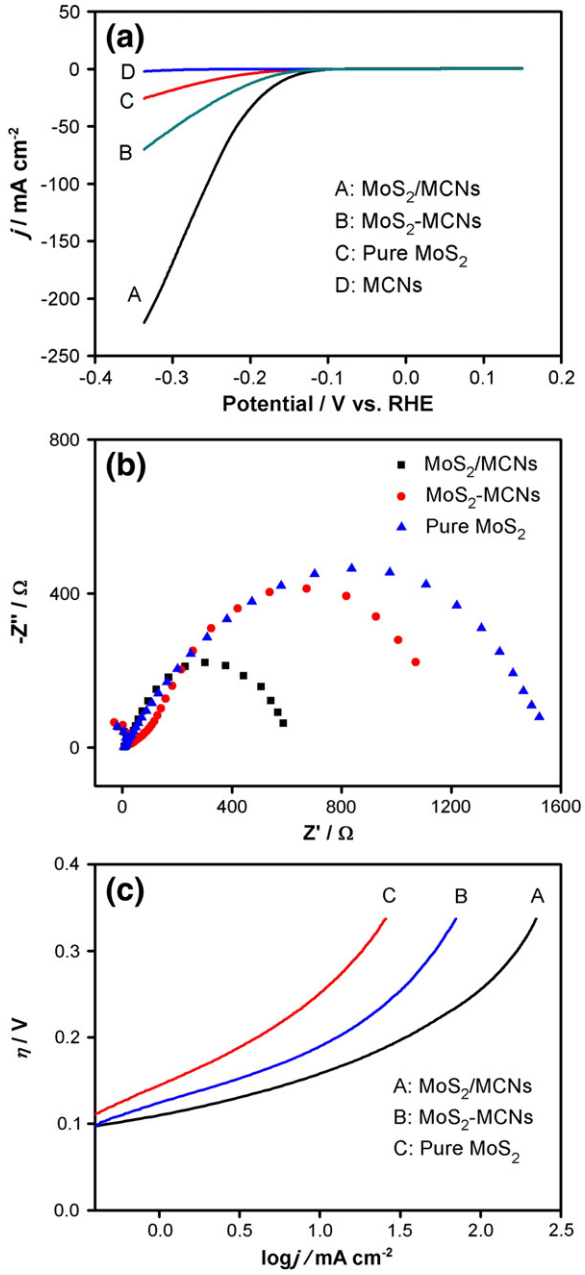

Fig. 3. (a) LSV polarisation curves for GCEs modified with (A) MoS_2/MCNs, (B) a mixture of MoS_2 and MCNs, (C) pure MoS_2 and (D) MCNs in 0.5 M H_2SO_4; scan rate: 2 mV/s. (b) Electrochemical impedance spectra at $\eta = 100$ mV and (c) Tafel plots for GCEs modified as indicated.

electrode displayed good stability towards HER during the 100 successive scans in 0.5 M H_2SO_4.

3.3. The mechanism of HER at the MoS_2/MCNs-modified electrode

The overall HER reaction occuring at an MoS_2 modified electrode surface in acidic media (Eq. (1)) may theoretically proceed via Volmer–Heyrovsky (Eq. (2) and (3)) or Volmer–Tafel mechanistic pathways (Eq. (2) and (4)),

$$2H_3O^+ + 2e^- \underset{k_-}{\overset{k}{\rightleftharpoons}} 2H_2O + H_2 \quad (1)$$

$$H_3O^+ + S + e^- \underset{k_{V-}}{\overset{k_V}{\rightleftharpoons}} H_2O + S - H \quad (2)$$

$$S - H + H_3O^+ + e^- \underset{k_{H-}}{\overset{k_H}{\rightleftharpoons}} H_2 + S + H_2O \quad (3)$$

$$2S - H \underset{k_{T-}}{\overset{k_T}{\rightleftharpoons}} 2S + H_2 \quad (4)$$

where S denotes a catalytic edge site and S–H denotes a hydrogen atom adsorbed at the site. The initial adsorption of the proton to form adsorbed hydrogen (Volmer) is generally considered to be fast, while the subsequent hydrogen desorption step (either Heyrovsky or Tafel) is typically rate limiting [8]. In this sense, it is clear that the binding energy of the adsorbed hydrogen intermediate is key, i.e., an optimum is necessary such that the intermediate is neither too tightly (desorption limiting) or loosely (adsorption limiting) bound. As yet, a general consensus has not been reached on the predominant HER mechanism at MoS_2 modified electrodes; however, DFT calculations of the hydrogen binding energy by Norskov calculated the fractional surface coverage of adsorbed hydrogen (θ) to be 0.25 on MoS_2 edge sites [5,7]. Such a value for θ supports an electrochemical desorption orientated Volmer–Heyrovsky mechanism taking precedent over recombination desorption via a Volmer–Tafel reaction pathway.

Herein, Tafel plots for MoS_2/MCNs, MoS_2-MCNs, and pure MoS_2 modified GCEs are shown in Fig. 3c. The Tafel slope for MoS_2/MCNs-GCEs, determined at low potentials, was ~41 mV/decade suggesting that HER takes place via a rapid Volmer reaction (Eq. (2)) followed by a rate-determining Heyrovsky step (Eq. (3)). The relatively low Tafel slope at low potentials is in line with MoS_2/graphene modified GCEs [16].

4. Conclusion

Ordered mesoporous carbon nanospheres provided an ideal matrice for in situ mediated growth of MoS_2 nanoparticles. The obtained MoS_2/MCNs was found to be a highly efficient catalyst for the electrocatalytic production of H_2 exhibiting a low overpotential and a high current density. The excellent catalytic activity observed was attributed to the design of the catalyst, which (a) maximised of the amount of edges per mole of MoS_2 immobilised on the electrode surface and (b) allowed optimisation of the conductivity to each MoS_2-edge present thereby improving the electronic contact between the active sites and the underlying electrode.

Acknowledgement

This work was supported by NSFC 20925517 and SKLEAC201101. The authors thank Professor W.B. Cai for helpful discussions.

References

[1] N.S. Lewis, D.G. Nocera, Proceedings of the National Academy of Sciences of the United States of America 103 (2006) 15729.
[2] J.A. Turner, Science 305 (2004) 972.
[3] N.S. Lewis, Science 315 (2007) 798.
[4] N.M. Marković, B.N. Grgur, P.N. Ross, The Journal of Physical Chemistry. B 101 (1997) 5405.
[5] B. Hinnemann, P.G. Moses, J. Bonde, K.P. Jørgensen, J.H. Nielsen, S. Horch, I. Chorkendorff, J.K. Nørskov, Journal of the American Chemical Society 127 (2005) 5308.
[6] J. Greeley, T.F. Jaramillo, J. Bonde, I.B. Chorkendorff, J.K. Norskov, Nature Materials 5 (2006) 909.
[7] T.F. Jaramillo, K.P. Jorgensen, J. Bonde, J.H. Nielsen, S. Horch, I. Chorkendorff, Science 317 (2007) 100.
[8] E. Skulason, G.S. Karlberg, J. Rossmeisl, T. Bligaard, J. Greeley, H. Jonsson, J.K. Norskov, Physical Chemistry Chemical Physics 9 (2007) 3241.
[9] D.V. Esposito, J.G. Chen, Energy & Environmental Science 4 (2011) 3900.
[10] H. Tributsch, J.C. Bennett, Journal of Electroanalytical Chemistry 81 (1977) 97.
[11] A.B. Laursen, S. Kegnæs, S. Dahl, I. Chorkendorff, Energy & Environmental Science 5 (2012) 5577.
[12] D. Merki, S. Fierro, H. Vrubel, X. Hu, Chemical Science 2 (2011) 1262.
[13] J. Kibsgaard, J.V. Lauritsen, E. Lægsgaard, B.S. Clausen, H. Topsøe, F. Besenbacher, Journal of the American Chemical Society 128 (2006) 13950.
[14] Q. Wang, J. Li, Journal of Physical Chemistry C 111 (2007) 1675.

[15] K. Chang, W. Chen, Chemical Communications 47 (2011) 4252.
[16] Y. Li, H. Wang, L. Xie, Y. Liang, G. Hong, H. Dai, Journal of the American Chemical Society 133 (2011) 7296.
[17] C. You, Y. Xuewu, Y. Wang, S. Zhang, J. Kong, D. Zhao, B. Liu, Electrochemistry Communications 11 (2009) 227.
[18] C. You, X. Yan, J. Kong, D. Zhao, B. Liu, Electrochemistry Communications 10 (2008) 1864.
[19] Y. Fang, D. Gu, Y. Zou, Z. Wu, F. Li, R. Che, Y. Deng, B. Tu, D. Zhao, Angewandte Chemie (International Ed. in English) 49 (2010) 7987.